Kinetic Effects of Alcohol Addition on the Anodic Behavior of Silicon in Acid Fluoride Media

Sandro Cattarin* and Marco M. Musiani

Istituto per l'Energetica e le Interfasi (IENI) - CNR, Corso Stati Uniti, 4 35127 Padova, Italy

Received: October 7, 2005; In Final Form: December 9, 2005

The anodic dissolution of silicon in acid solutions of ammonium fluoride is investigated in aqueous and water−alcohol media by rotating disk voltammetry and impedance spectroscopy. The voltammograms recorded in water−alcohol media show, in comparison to water, the following effects: an increase of the dissolution currents measured at pH > 2 and an opposite effect at pH < 2; a distortion of the curve, with a relative increase of the characteristic currents in the region of low applied potentials, indicating easier dissolution of the "wet" oxide forming under those conditions; a shift of the maximum of the current−pH curves from about pH 3 in water to about pH 4 in 50% ethanol v/v. Analysis of impedance data at pH values 4−5 in water and water−ethanol media show similar dependence on potential for the parameters C_{hf} (high-frequency capacitance) and $R_{hf}I$ (R_{hf} is a high-frequency resistance and I is the steady state current), suggesting the formation of oxide films with similar properties. The marked differences of anodic behavior in the two types of media are discussed and explained in terms of the effects of alcohol addition on the speciation equilibria of hydrofluoric acid and on the kinetic rate constants of dissolution of the surface oxide layer.

1. Introduction

The anodic behavior of silicon in aqueous fluoride solutions has been extensively investigated in the last two decades, to improve the fundamental understanding of the oxidation phenomena[1−3] and to gain better control over processes of potential technological interest like electrochemical etching,[4] porous silicon formation,[5−8] oxide growth,[9−12] electropolishing,[13−16] and the preparation of hydrogen-terminated surfaces.[17]

When making porous silicon, several authors prefer using water−alcohol solutions (containing typically methanol[8] or ethanol[7]) to obtain nice uniform porous layers. The reason for this is that silicon dissolution at the appropriate potential is accompanied by hydrogen gas evolution and the surfactant action of alcohol promotes the detachment of tiny bubbles at an early stage of their formation, reducing the problems of nonhomogeneous treatment resulting from the growth of large bubbles sticking on the surface or the disruption of electric contact inside the pores.[7] Unlike most of the other surfactants, alcohol is easily removed by drying.

The effect of alcohol addition to the fluoride medium on the anodic behavior of Si has not received, to the best of our knowledge, a thorough investigation in the literature. The possible reason for this is that it is mostly regarded as a detail of a recipe, with a limited physical effect and no significant chemical action. However, alcohol addition should not be regarded as innocent, since the changes of the dielectric constant and acid−base properties of the solvent may modify both the equilibria of hydrofluoric species in solution[18,19] and the kinetic constants of dissolution processes: hence, the chemical rate of SiO_2 dissolution[20−22] and the overall kinetics of anodic processes[15] may change markedly.

In a recent preliminary account,[23] we have anticipated the main observations of voltammetric investigations, in particular the enhancement of Si dissolution caused by the addition of ethanol at a pH > 2 and a shift of the maximum in the current−pH curves from pH 3 in water to about pH 4 in water−ethanol; we report in this paper an extended investigation, the discussion of a kinetic model, and the study of impedance response. Reported experiments are focused on solutions of HF/NH_4F, a classical medium for wet etching and surface conditioning of silicon.[24−26] The differences of anodic behavior in purely aqueous and water−alcohol solutions are discussed and interpreted considering changes in the speciation equilibria in solution and in the rate constants of oxide dissolution by active hydrofluoric species.

2. Experimental Section

Electrodes were prepared from (100) p-Si wafers with a thickness of 525 ± 20 μm and a resistivity of about 10 Ω cm, mirror polished on one side. A p+ layer was formed on the back by B implantation. Square pieces were cut from the wafer and shaped into disks. The backside was then contacted with Indium−Gallium eutectic and fixed with silver epoxy to the top of a brass rod sealed in a Vespel cylinder. A final sealing with epoxy resin led to rotating disk electrodes (RDE) with surface areas in the range 0.60 −0.80 cm^2.

The electrolytes were prepared from water deionized by a Millipore Milli-RO system, commercial alcohols pro analysis grade (Fluka), and high purity chemicals (Fluka or Aldrich). Preliminary fluoride solutions were prepared by dilution of a 40% NH_4F commercial solution (BDH Aristar). Aqueous stock solutions were prepared from (i) a solution containing support electrolyte and buffer, of a pH adjusted under control at the pH meter and (ii) a fluoride solution of the same pH adjusted under control with pH-indicator strips. The aqueous stock solutions contained the following: 1.0 mol L^{-1} NH_4Cl as a support electrolyte; up to 0.2 mol L^{-1} NH_4F; 0.4 mol L^{-1} choloroacetic acid (pH 2−3) or acetic acid (pH 4−5) as a buffer.

* E-mail address: s.cattarin@ieni.cnr.it.

10.1021/jp055714g CCC: $33.50
Published on Web 01/12/2006

Electrochemical experiments were mostly performed in pairs, one in aqueous and one in water−alcohol medium. Solutions were in turn prepared according to two different procedures.

Procedure I was straightforward: 50 mL of the stock solution was diluted to 100 mL by simple mixing with either (a) water, to obtain the usual aqueous solution or (b) alcohol in the desired amount and water as necessary to bring the solution to volume, to obtain water−alcohol solutions. The pH, estimated with indicator strips, did not vary significantly upon mixing the stock solution with water, whereas marked variations were observed after mixing with alcohol.

In procedure II, the pH of each pair of solutions prepared by dilution of the stock solution with water or alcohol was finally adjusted to the same value. Since the pH varied (increased) significantly only upon dilution with alcohol, pH correction with HCl was actually required only for water−alcohol solutions.

The alcohol amount was estimated by volume: for example, a 50% v/v water−alcohol solution contained 50 mL of alcohol in a total volume of 100 mL. A typical composition of the operating solutions was the following: 0.5 mol L^{-1} NH_4Cl; up to 0.1 mol L^{-1} NH_4F; 0.2 mol L^{-1} chloroacetic or acetic acid. The most acidic solutions (pH 0 and pH 1) contained HCl instead of the organic acid. The use of a fairly large concentration of NH_4Cl in all electrolytes—except that at pH 0—aimed at providing similar ionic strength and a rather constant concentration of NH_4^+, which is known to influence significantly the anodic current.[27,28]

The electrochemical setup consisted of a plastic cell and a classical three-electrode arrangement. The working electrode was polished prior to experiments with diamond paste down to 0.25 μm grain size and was then polarized for several minutes in the electropolishing regime until a steady dissolution current was attained. The counter electrode was a Pt wire with a surface of about 10 cm^2. A saturated calomel electrode (SCE) was used as a reference, and potentials are referred to it. The SCE was inserted in a bridge, filled with the same solution as in the cell but free of fluoride and protected from the cell solution with a Teflon tape (except for the septum tip ensuring electric contact) to minimize the contact of glass and fluoride.

The cyclic voltammetries were recorded with an Amel electrochemical apparatus (potentiostat and function generator) equipped with a multipurpose laboratory interface (Vernier) allowing data acquisition in digital form. Alternating current (ac) impedance experiments were performed using a Solartron 1254 frequency response analyzer and a Solartron 1286 electrochemical interface, both computer driven by the commercial software FRACOM.

3. Results

3.1. Behavior in Aqueous and Water−Alcohol Media Containing the Same Solutes. In this section, we discuss pairs of experiments performed in solutions prepared according to procedure I, namely, by simple mixing of the stock solutions with either water or alcohol, allowing the spontaneous pH variations.

A first pair of voltammetric experiments (Figure 1) is made in two solutions obtained by diluting a stock solution of pH 3.0. Figure 1a shows the voltammogram recorded in the aqueous solution (pH ≅ 3.0); the pattern shows a first sharp peak and a second broad peak, followed by a region of current oscillations.[12−17] Four characteristic current densities, j_1, j_2, j_3, and j_4, may be identified as proposed by Chazalviel and collaborators.[14] The voltammogram recorded in a water−alcohol solution containing 50% v/v of ethanol (pH ≅ 3.8) is reported in Figure 1b and shows, in comparison with Figure 1a, a general increase of the current values, more marked for j_1 and j_2, leading to a curve distortion.

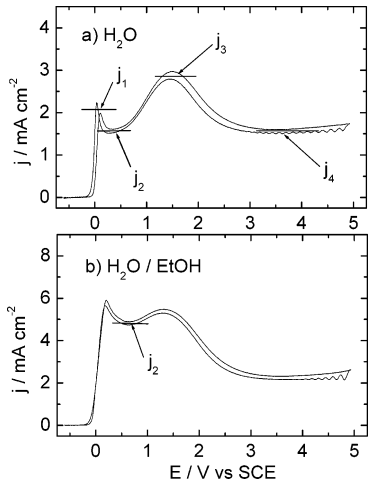

Figure 1. Cyclic voltammograms (20 mV s^{-1}) recorded at a RDE (900 rpm). The solutions used are as follows: (a) aqueous (pH ≅ 3.0) and (b) water−alcohol, 50% v/v ethanol (pH ≅ 3.8) prepared according to procedure I, diluting an aqueous stock solution at pH 3.0. The composition of experimental solutions is as follows: 0.5 mol L^{-1} NH_4Cl, 0.2 mol L^{-1} chloroacetic acid, and 0.1 mol L^{-1} NH_4F. The characteristic current densities j_1, j_2, j_3, and j_4 are indicated in part a.

For the sake of comparison, a few experiments are made in the presence of alkali metal cations, using alkali metal chlorides besides (or instead of) NH_4Cl as the supporting electrolyte; the interest is merely fundamental, since in technological treatments alkali cations are dangerous contaminants of silicon. Experiments show under most conditions phenomena of dissolution/precipitation: for example, the addition of KCl, RbCl, and CsCl in the order of 0.1 mol L^{-1} to the solutions of Figure 1 leads to voltammetric hysteresis indicating progressive passivation (the current in the backward scan is lower or much lower than in the forward scan), and the electrode at the end of the polarization experiment is covered by a whitish material. Most likely, the phenomena of precipitation of insoluble hexafluorosilicates, already observed in water,[27,28] tend to be more pronounced in water−alcohol. Further experiments are performed in solutions containing only NH_4^+ and give no evidence of precipitation of insoluble salts.

The investigation is then extended to the other alcohols which are fully miscible with water. Curves similar to that obtained for ethanol are recorded also operating in media containing 50% v/v methanol or *n*-propanol; in these cases too, the solution pH is estimated at about 3.8. The dependence of current on rotation rate is shown for j_2 in the Koutecky−Levich plots of Figure 2. In every case, the relation between the current and the rotation rate Ω is of the type

$$j^{-1} = j_k^{-1} + j_d^{-1} = j_k^{-1} + B\Omega^{-1/2} \qquad (1)$$

where j_d is the term depending on the mass transport and j_k is the kinetic current in the absence of transport limitations, extrapolated for $\Omega^{-1/2} \rightarrow 0$. A strong increase of j_{2k} is observed on going from water (1.7 mA cm^{-2}) to the water−alcohol solutions, that show values in the range 7−10 mA cm^{-2} with a maximum in correspondence with ethanol. Ethanol is used in all further experiments.

Figure 3 shows the results obtained in solutions prepared by mixing an aqueous stock solution of pH 4.0 (1.0 mol L^{-1} NH_4Cl; 0.2 mol L^{-1} NH_4F; 0.4 mol L^{-1} acetic acid) with water

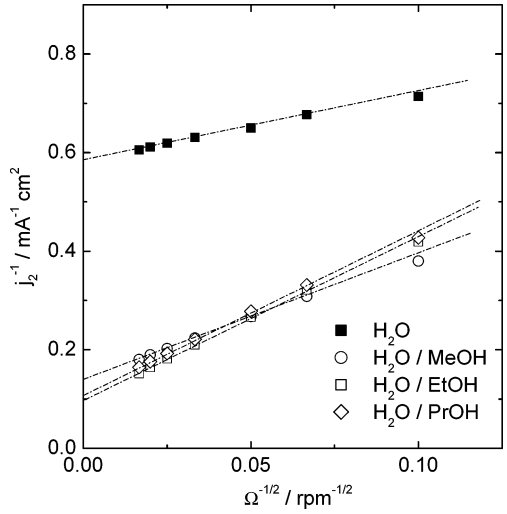

Figure 2. Koutecky−Levich plots obtained for electrodissolution in aqueous (pH ≅ 3.0) and water−alcohol media (pH ≅ 3.8) prepared as in Figure 1.

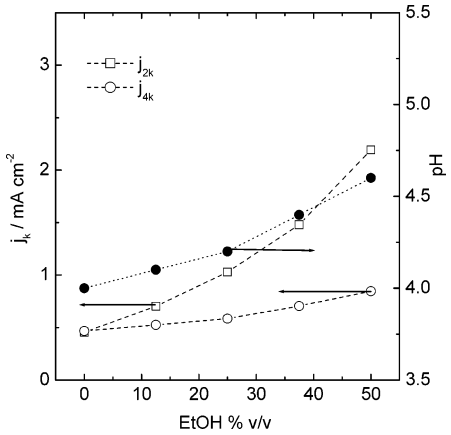

Figure 3. pH (full dots, right scale) and kinetic current densities j_{2k} and j_{4k} (empty symbols, left scale) measured in solutions obtained by procedure I, diluting an aqueous stock solution at pH 4.0 with water and ethanol in different volume ratios. The composition of experimental solutions is as follows: 0.5 M NH_4Cl, 0.1 M NH_4F, and 0.2 M acetic acid.

and various volumes of ethanol up to 50% v/v, for a same final concentration of electrolytes in all cases. On increasing the alcohol fraction, an increase of both pH (Figure 3, full dots) and j_k is observed (Figure 3, empty symbols), more pronounced for j_{2k} than for j_{4k} according to a progressive distortion in shape of the $j-E$ curve.

Figure 4 shows the dependence of j_{2k} on pH observed in a series of experiments performed in solution pairs obtained upon mixing various aqueous stock solutions of pH between 0 and 5.0 with 50% v/v of either water or ethanol. It is shown that in all cases alcohol addition causes a pH increase: minor for the most acid solutions and marked at pH > 2. The current is higher in water−alcohol solutions at pH > 2 but not at pH < 2 where the opposite effect is observed.

The points relevant to aqueous solutions show a maximum value of j_{2k} at about pH 3.0, in agreement with previous reports.[14,15] For water−alcohol solutions, the maximum is shifted to pH ≅ 3.8 (experiments of Figure 1).

3.2. Behavior in Aqueous and Water−Ethanol Solutions of the Same pH. In this section, we discuss pairs of experiments performed in aqueous and water−alcohol solutions whose pH is adjusted to the same value (procedure II). Typically, the

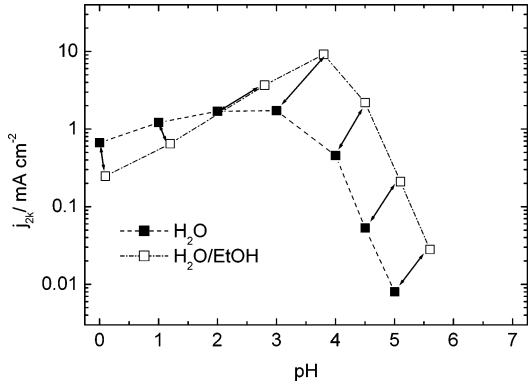

Figure 4. Dependence of the kinetic current density j_{2k} on pH for pairs of aqueous solutions (full squares) and water−alcohol solutions (50% v/v, empty squares) obtained by diluting the suitable stock solution with water or ethanol by procedure I. The composition of experimental solutions is as follows: 0.5 mol L^{-1} NH_4Cl and 0.1 mol L^{-1} NH_4F. The buffer used is as follows: 0.2 mol L^{-1} chloroacetic or acetic acid at pH ≥ 2; HCl in a suitable amount at pH 1 and pH 0. Each solutions pair is connected by an arrow.

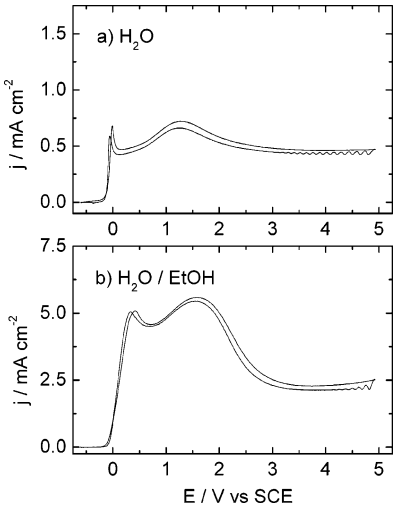

Figure 5. Cyclic voltammograms recorded at a RDE (900 rpm) in two solutions of the same pH ≅ 4.0 prepared by procedure II: (a) aqueous solution (scan rate 5 mV s^{-1}); (b) water−alcohol solution with 50% v/v ethanol (scan rate 20 mV s^{-1}). The composition of experimental solutions is as follows: 0.5 mol L^{-1} NH_4Cl, 0.1 mol L^{-1} NH_4F, and 0.2 mol L^{-1} acetic acid.

water−alcohol solution contains, besides a different solvent, a small additional amount of HCl.

The voltammograms recorded in aqueous and water−alcohol solution (50% v/v EtOH) at pH 4.0 are reported in Figure 5a and b, respectively. The $j-E$ curve recorded in the latter case shows a current markedly higher on the whole range of potentials and especially in the region of low applied potentials: j_{2k} (value estimated by Koutecky−Levich analysis) increases by a factor of about 20 as compared to the aqueous solution.

The relation between the kinetic component j_k of the current density and the analytical fluoride concentration c_F has been investigated in aqueous solutions by the group of Chazalviel,[14] who found a relation of the type $j_k \propto c_F^{\alpha}$, with $\alpha \cong 2.0-2.5$, for solutions of same pH in the range 0−4. In two series of measurements at pH 3.0 over the concentration range c_F = 0.020−0.200 mol L^{-1}, we have found values of $\alpha \cong 2.0$ for the aqueous solutions and $\alpha \cong 2.2-2.3$ for water−alcohol media; the difference appears significant, but the values are still in the same range.

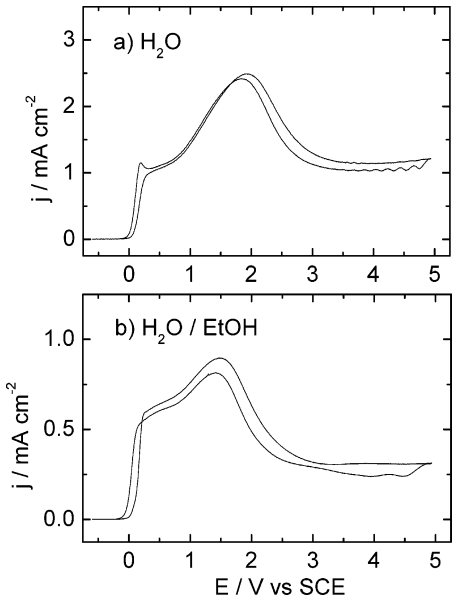

Figure 6. Cyclic voltammograms recorded at a RDE (900 rpm) in solutions of the same pH ≅ 1.0 prepared by procedure II: (a) aqueous solution (scan rate 10 mV s^{-1}); (b) water−alcohol solution with 50% v/v ethanol (scan rate 10 mV s^{-1}). The composition of experimental solutions is as follows: 0.5 mol L^{-1} NH_4Cl, 0.1 mol L^{-1} NH_4F, and HCl ≅ 0.2 mol L^{-1}.

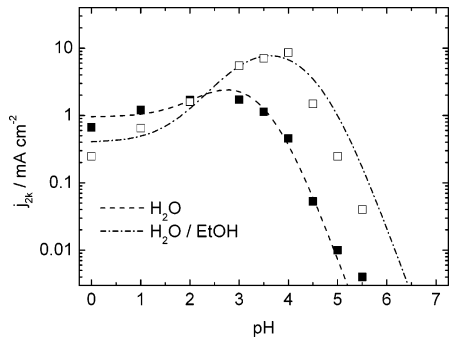

Figure 7. Dependence of the kinetic current density j_{2k} on pH. Experiments were performed in pairs, in aqueous and water−alcohol solutions (50% v/v ethanol) of same pH prepared according to procedure II. The dashed (water) and dashed−dotted (water−alcohol) lines show the dependence of j_{2k} on pH according to eq 5. The parameters used in the calculation are as follows: for aqueous solutions $nFk_1 = 9.5 \times 10^4$ A cm^4 mol^{-2}, $nFk_2 = 7.0 \times 10^6$ A cm^4 mol^{-2}, $nFk_3 = 3.7 \times 10^6$ A cm^4 mol^{-2}; for water−alcohol solutions $nFk_1' = 4.0 \times 10^4$ A cm^4 mol^{-2}, $nFk_2' = 1.4 \times 10^7$ A cm^4 mol^{-2}, $nFk_3' = 7.4 \times 10^6$ A cm^4 mol^{-2}.

The voltammograms presented in Figure 6 show the effect of alcohol addition in the region of low pH: a current decrease affects the entire curve, but in a more pronounced way, it affects the region of j_4, leading to a distortion of the curve shape again similar to that observed in Figure 1.

Figure 7 summarizes the results obtained in a series of parallel experiments over the entire range of acid pH, from 0 to about 6. The results—in good agreement with those in Figure 4—show that at pH > 2 the j_{2k} values are always larger in water−alcohol solution than in aqueous solution; on the other hand, the effect is inverted at pH < 2. The maximum of j_{2k} is located around pH 3.0 in aqueous solutions and occurs in water−alcohol at a higher pH, around 4.0.

3.3. Impedance Investigations. Impedance experiments are performed in aqueous and water−alcohol media prepared with procedure I from a stock solution of pH 4.0. The selected pair of experiments permits operation in a current range warranting quick attainment of stationary conditions and not too fast electrode consumption. The spectra are recorded only from the upper frequency limit of 63 kHz down to 1 Hz; the range of low frequencies is not explored to limit the duration of the experiments and the associated slow evolution of the system, considering that our aim is to show the dependence on potential of the high frequency parameters associated with the properties of the Si/electrolyte interface or of the oxide layer present on the surface.

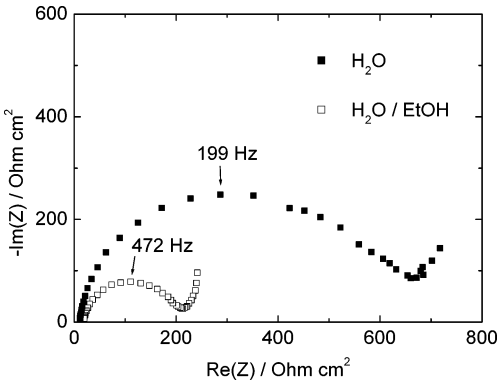

Figure 8. Impedance plots recorded at a p-Si RDE (900 rpm) at E = 0.450 V in aqueous and water−alcohol media. The (a) aqueous (pH ≅ 4.0) and (b) water−alcohol (50% v/v ethanol, pH ≅ 4.6) solutions were prepared according to procedure I, diluting an aqueous stock solution at pH 4.0. The composition of the final solution was as follows: 0.5 mol L^{-1} NH_4Cl, 0.1 mol L^{-1} NH_4F, and 0.2 mol L^{-1} acetic acid.

Figure 8 shows the Nyquist plots recorded in the two media at the applied potential E = 0.450 V, corresponding to the current j_2 in the water−ethanol medium (a comparable shape is maintained at more positive potentials). Under these conditions, the current is 2−3 times larger in water−ethanol than in water, and this influences the size of the observed high frequency loop. This is associated with a semiconductor polarized under accumulation and covered by a hydroxide/oxide layer and includes, therefore, unresolved contributions from the Helmholtz double layer and the oxide layer, with the latter progressively dominating as the oxide grows. From the analysis of this loop, one obtains the high frequency resistance R_{hf} and the high frequency capacitance C_{hf}. Actually, at potentials negative to 0.1 V, the portion of a further loop appears at the highest frequencies; this loop (better defined at more negative potentials) is associated with a space charge capacitance (the flatband potential occurs at about 0.10−0.15 V for p-Si in similar media),[29] and we shall not deal with it. Considering again Figure 8, in comparison with the spectrum recorded in water, that obtained in the water−alcohol solution provides the following: a larger electrolyte resistance R_Ω; a smaller high frequency resistance R_{hf}; a very similar capacitance $C_{hf} \cong 1.5$ μF cm^{-2}.

Two series of spectra are recorded, one in each medium, every 25−50 mV in the peak region and every 500 mV at potentials positive to 0.5 V. Figure 9b shows the dependence on potential of the parameter $R_{hf}I$ (I being the stationary current). Values between 15 and 30−40 mV are estimated at the foot of the peak; these values, around $RT/F \cong 25.7$ mV, are rather typical of a reaction at a bare (H-terminated) semiconductor surface, controlled by carrier supply (p-Si under mild depletion), when all variations of potential drop occur in the space charge layer.[30] The $R_{hf}I$ parameter shows, then, the following: a steep increase at potentials positive to the current maximum, where the surface is known to get progressively passivated by oxide species; a plateau extending over the region of the second current maximum j_3; a linear increase with a slope of 0.19−0.20 in the

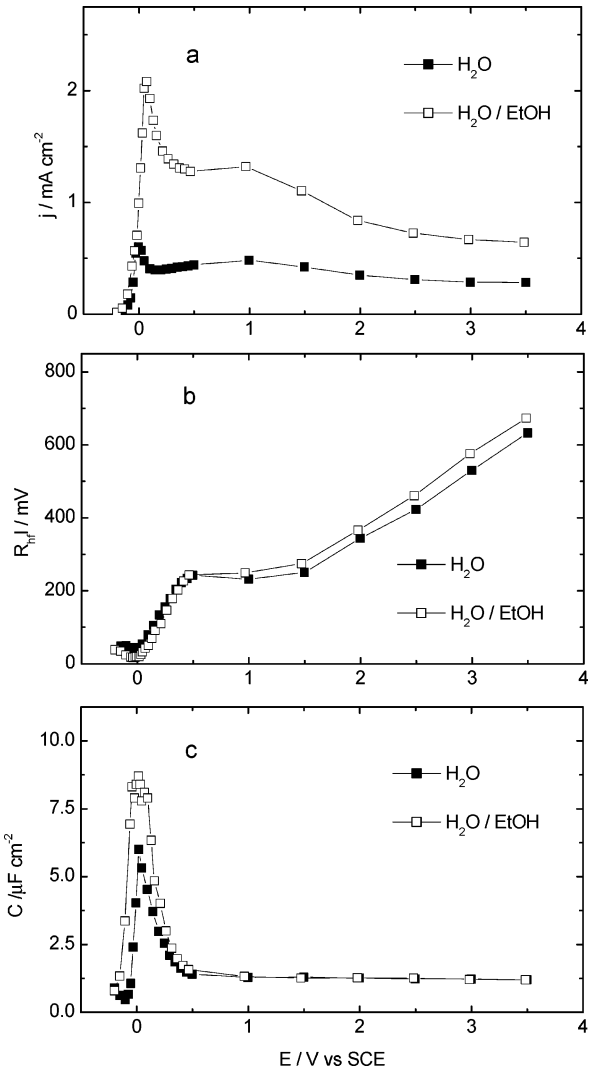

Figure 9. Results of two parallel series of impedance measurements performed in aqueous and water−alcohol media under the same conditions of Figure 8 and showing, as a function of electrode potential, (a) stationary currents, (b) $R_{hf}I$, and (c) capacitance.

region above 1.5 V. The latter dependence is typical of film growth under a high field migration mechanism.[16,31]

The data of Figure 9c show the dependence on potential E of the electrode capacitance. It is apparent that the capacitance values show a maximum in the potential region of the current peak j_1 and then decrease assuming at potentials positive to 1.5 V values very slightly decreasing with potential. The capacitance increase at potentials positive to current onset may be attributed to a surface change and/or to some surface roughening. The capacitance remains fairly large in the potential region of the peak until formation of a passivating oxide layer which causes a drop of capacitance (and of current). The trends are qualitatively similar in aqueous and water−alcohol solutions; the capacitance values are very close for the two media at potentials above 1 V, but a significant difference is observed around 0.0 V, where the peak in water−alcohol solutions is higher and wider.

4. Discussion and Conclusions

Investigations in aqueous and water−alcohol media show both important differences and similarities: (i) modification of the voltammetric patterns (Figures 1 and 5); (ii) increase or decrease of dissolution currents, depending on the solution pH (Figures 5 and 6); (iii) shift of the maximum of the current−pH curves, from about pH 3 in water to pH 4 in 50% ethanol v/v (Figure 7); (iv) similar dependence of the parameters $R_{hf}I$ and C_{hf} on potential (Figure 9). We shall consider them in turn.

The surface conditions of a Si anode polarized in acid fluoride media is known to change with potential.[32] Sweeping the potential of an etched electrode positive to an open circuit, the surface is hydrogen-terminated in the Tafel region preceding j_1, becomes covered by a wet oxide in the potential region between j_1 and j_3, and is finally covered by a compact dry oxide, more similar to a thermal oxide, going positive to j_3 into the electropolishing plateau. At the oxide covered electrode, electrodissolution requires oxide formation at the Si/oxide interface and its chemical dissolution at the oxide/solution interface by the species HF and HF_2^- (F^- is inert).[20−22] Hence, the distortion of the voltammetry observed at pH > 2 indicates that the active/passive transition occurs in water−alcohol at higher current densities and that the "wet" oxide forming at moderate positive potentials dissolves faster (Figure 1 and 5); less marked are the differences for the compact "dry" oxide forming at higher potentials, which behaves in a more similar way in the two media. At pH < 2, the general effect on current is opposite but the curves show a similar distortion.

Concerning changes in the dissolution currents, we must consider two possible effects of alcohol: modification of the equilibria in solution, altering the concentrations of fluoride species HF and HF_2^-, and changes in the kinetic constants of the processes of oxide dissolution, resulting, e.g., from variations of the activation energies of the key steps. No significant direct dissolution of silica by ethanol is expected on the basis of the known silica chemistry, since processes such as esterification forming Si−O−C bonds require anhydrous media and high temperatures.[33]

The dissociation equilibria of weak acids are markedly affected by the addition of organic solvents to water,[34] a problem extensively treated for the case of water−alcohol mixtures.[35] The speciation equilibria of fluoride species, namely

$$HF \leftrightarrow H^+ + F^- \qquad K_1[HF] = [H^+][F^-] \tag{2}$$

$$HF_2^- \leftrightarrow HF + F^- \qquad K_2[HF_2^-] = [HF][F^-] \tag{3}$$

$$[HF] + 2[HF_2^-] + [F^-] = c_F \tag{4}$$

are defined by c_F (the total fluoride concentration) and the dissociation constants K_1 and K_2, for which there are in the literature several values. In a previous publication, we referred to those adopted by Judge,[20] but here, we shall refer to those proposed by Luxemberg and Kim,[19] which are similar and include both water and water−ethanol mixtures. From their tables, we take the values (at 25 °C): $K_1 = 6.7 \times 10^{-4}$ mol L^{-1} and $K_2 = 0.200$ mol L^{-1} in pure water. The data relevant to water−ethanol have been estimated for different ionic strengths I_s and show an increase of the constants in solutions of higher ionic strength I_s; we have used the values relevant to $I_s = 0.1$ mol L^{-1}, the maximum available I_s, which is still much below those of our operating conditions. The values interpolated for a solution containing 44% wt/wt ethanol, corresponding to our 50% v/v mixtures, are $K_1' = 1.11 \times 10^{-4}$ mol L^{-1} and $K_2' = 0.084$ mol L^{-1}; considering the effect of the ionic strength, the real constants are certainly higher. The two couples of constants are used to calculate the speciation diagrams of Figure 10a and b, which provide a first qualitative explanation of why active dissolution extends to higher pH in the water−alcohol me-

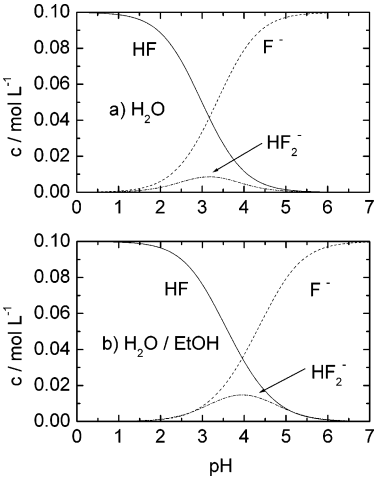

Figure 10. Speciation diagrams of the fluoride species (total fluoride concentration $c_F = 0.1$ mol L^{-1}) in (a) aqueous solutions, $K_1 = 6.76 \times 10^{-4}$ mol L^{-1}, $K_2 = 0.200$ mol L^{-1} and (b) water−alcohol solutions (50% ethanol v/v), $K_1' = 1.11 \times 10^{-4}$ mol L^{-1}, $K_2' = 0.084$ mol L^{-1}.

dium: the dissociation of HF shifts to higher pH ($pK_1' > pK_1$), and so does the maximum concentration of the species HF_2^-, which increases in size. Since HF and especially HF_2^- are the active species for SiO_2 dissolution,[15,20−22] the maximum dissolution current shifts to higher pH. To reproduce accurately the dependence of j_{2k} on pH, we adapt the scheme used in a previous paper for aqueous solutions,[15] assuming that the stationary current is imposed by the rate of chemical dissolution of the SiO_2 surface film in parallel paths involving HF and HF_2^-. The overall j_{2k} is obtained as the sum of three contributions compatible with the experimental second-order kinetics ($j_k \propto c_F^{\alpha}$ with $\alpha \cong 2$):

$$j_{2k} = nFk_1[HF]^2 + nFk_2[HF_2^-]^2 + nFk_3[HF][HF_2^-] \quad (5)$$

where $n \cong 4$ represents the number of Faradays consumed for the oxidation of a silicon mole,[36] the concentrations are those in the bulk of the solution, and k_1, k_2, and k_3 are kinetic rate constants.

The curves in Figure 7 show the calculated dependence of j_{2k} on pH for $c_F = 0.1$ mol L^{-1}, using different sets of constants for the cases of water and water−alcohol. In the case of aqueous solutions, a good match with experimental data is obtained using constants similar to those used in ref 15, just adapted to account for the different conditions (values attributed to the dissociation constants K_1 and K_2; point of the $j-E$ curve at which current is read; concentration of ammonium, affecting the dissolution current). The set of adopted values is the following: $nFk_1 = 9.5 \times 10^4$ A cm^4 mol^{-2}; $nFk_2 = 7.0 \times 10^6$ A cm^4 mol^{-2}; $nFk_3 = 3.7 \times 10^6$ A cm^4 mol^{-2}.

Concerning water−alcohol media, results cannot be reproduced by the mere change of the speciation equilibria shown in Figure 10 and we must assume also a variation of the kinetic constants k_1, k_2, and k_3. In principle, any tuning of eq 5 required to simulate the experimental findings contains information on the changes of mechanism induced by alcohol addition. However, the presence of alcohol may influence the process of oxide formation/dissolution in many ways, e.g., by altering the activity of water, the compactness of the formed anodic oxide and its surface wettability, the point of zero charge of silica[33] and the electric field profile at the Si/SiO_2/electrolyte junction, the surface concentration of species active in promoting dissolution and/or their reactivity, and the solvation of intermediates and products. What is observed in our experiments is the overall effect of several mechanistic contributions, and since there is not a sufficient basis for a detailed analysis, we will maintain the discussion at a phenomenological level which appears adequate for the scope of the present paper.

The current decrease induced by ethanol addition at pH values 0−2 is consistent with a decrease of k_1 and corresponds to the decrease of chemical etch rate already reported in the literature for HF solutions[22] and attributed to an increasing activation energy on increasing the ethanol content for the reaction of the neutral species HF (or the dimer H_2F_2) with SiO_2. To reproduce the current increase in water−alcohol at pH > 2, we must assume, conversely, an increase in the kinetic constants k_2 and k_3, which should be related likewise to a decrease of activation energy for the reaction of SiO_2 with the charged species HF_2^-. The set of adopted values is as follows: $nFk_1' = 4.0 \times 10^4$ A cm^4 mol^{-2}; $nFk_2' = 1.4 \times 10^7$ A cm^4 mol^{-2}; $nFk_3' = 7.4 \times 10^6$ A cm^4 mol^{-2}. Comparison of experimental (points) and calculated values (line) in Figure 7 shows a rather good match but a systematic discrepancy at pH > 4. The latter would be reduced or even eliminated by using the (higher) dissociation constants K_i appropriate for our experimental ionic strength and by allowing the exponent in eq 5 to take values somewhat larger than 2.0—in agreement with experimental indications—but we prefer to leave things at this stage.

The information provided by our impedance investigations is the similar dependence of the $R_{hf}I$ and C_{hf} parameters on potential in the two media. The $R_{hf}I$ parameter (Figure 9b) shows a linear increase in the region above 1.5 V which allows, in the frame of the high field migration theory, the estimation of the film formation ratio:[31]

$$\frac{dx}{dE} = B\frac{d(R_{hf}I)}{dE} \quad (6)$$

where $B = zaF/RT$, z is the electric charge of the mobile ionic species, a is the half jump distance, F, R, and T have their usual meaning, and $F/RT = 38.92$ V^{-1}. The experimental slope of 0.19−0.20 corresponds, for $a = 2$ Å, to a formation ratio of ca. 30 Å V^{-1} for $z = 2$ (transport by oxygen vacancies) or 15 Å V^{-1} for $z = 1$ (transport by oxygen semivacancies[9]), in the range of typical literature values.[12,16] The fact that the slope is basically the same in the two media would indicate that the nature of the film is also very similar.

This is confirmed by comparison of the $C_{hf}-E$ curves (Figure 9c): the capacitance values at potentials above 1 V are very close for the two media, indicating that the compact dielectric film has similar thickness. A significant difference is conversely apparent in the region of low potentials since the peak around 0.0 V is higher and wider in water−alcohol solutions, suggesting a less efficient passivation by the wet oxide in the given conditions of lower water activity and the presence of an organic solvent.

We notice some sort of inconsistency between the linear increase of $R_{hf}I$ at $E > 1.5$ V (Figure 9b) and the almost constant value of C_{hf} in the same potential range (Figure 9c). A similar discrepancy has been already reported in the literature: capacitance measurements[12] show a rather constant value, whereas infrared data[37] indicate linear growth in thickness with the potential. The discrepancy is attributed[12] to the complex nature of the film, consisting of a thin dielectric inner layer, a central layer of defective dry oxide, and an outer layer of partially hydrated oxide, and to the fact that different techniques perform a different sampling of film properties. A similar type of explanation may hold also in our case, but the specific physical model is not obvious.

Concluding, analogies and differences of the anodic Si behavior in aqueous and water−alcohol solutions may be interpreted assuming formation of oxide films with similar properties but different dissolution rates. Most of the variations observed in water−alcohol medium as compared to water—extension of the pH dissolution range toward higher values, consistent shift of the current maximum, increase in its absolute value—may be basically explained by the changes in the speciation equilibria of acid fluoride and the change in the kinetic constants of oxide dissolution.

References and Notes

(1) Searson, P. C.; Zhang, X. G. *J. Electrochem. Soc.* **1990**, *137*, 2539.

(2) Blackwood, D. J.; Borazio, A.; Greef, R.; Peter, L. M.; Stumper, J. *Electrochim. Acta* **1992**, *37*, 889.

(3) Gerischer, H.; Allongue, P.; Costa Kieling, V. *Ber. Bunsen-Ges. Phys. Chem.* **1993**, *97*, 753.

(4) Lehmann, V.; Föll, H. *J. Electrochem. Soc.* **1990**, *137*, 653.

(5) Smith, R. L.; Collins, S. D. *J. Appl. Phys.* **1992**, *71*, R1.

(6) Lehmann, V. *Adv. Mater.* **1992**, *4*, 762.

(7) Searson, P. C.; Macaulay, J. M.; Prokes, S. M. *J. Electrochem. Soc.* **1992**, *139*, 3373.

(8) Xie, Y. H.; Hybertsen, M. S.; Wilson, W. L.; Ipri, S. A.; Carver, G. E.; Brown, W. L.; Dons, E.; Weir, B. E.; Kortan, A. R.; Watson, G. P.; Liddle, A. J. *Phys. Rev. B* **1994**, *49*, 5386.

(9) Chazalviel, J.-N. *Electrochim. Acta* **1992**, *37*, 865.

(10) Lewerenz, H. J. *Electrochim. Acta* **1992**, *37*, 847.

(11) Schmuki, P.; Böhni, H.; Bardwell, J. A. *J. Electrochem. Soc.* **1995**, *142*, 1705.

(12) Bailes, M.; Böhm, S.; Peter, L. M.; Riley, D. J.; Greef, R. *Electrochim. Acta* **1998**, *43*, 1757.

(13) Serre, C.; Barret, S.; Hérino, R. *J. Electrochem. Soc.* **1994**, *141*, 2049.

(14) Hassan, H. H.; Sculfort, J. L.; Etman, M.; Ozanam, F.; Chazalviel, J.-N. *J. Electroanal. Chem.* **1995**, *380*, 55.

(15) Cattarin, S.; Frateur, I.; Musiani, M.; Tribollet, B. *J. Electrochem. Soc.* **2000**, *147*, 3277.

(16) Frateur, I.; Cattarin, S.; Musiani, M.; Tribollet, B. *J. Electroanal. Chem.* **2000**, *482*, 202.

(17) Rappich, J.; Aggour, M.; Rauscher, S.; Lewerenz, H. J.; Jungblut, H. *Surf. Sci.* **1995**, *335*, 160.

(18) Broene, H. H.; de Vries, T. *J. Am. Chem. Soc.* **1947**, *69*, 1644.

(19) Luxemberg, P.; Kim, J. I. *Z. Phys. Chem.* **1980**, *121*, 187.

(20) Judge, J. S. *J. Electrochem. Soc.* **1971**, *118*, 1772.

(21) Verhaverbeke, S.; Teerlinck, I.; Vinckier, C.; Stevens, G.; Cartuyvels, R.; Heyns, M. M. *J. Electrochem. Soc.* **1994**, *141*, 2852.

(22) Garrido, B.; Montserrat, J.; Morante, J. R. *J. Electrochem. Soc.* **1996**, *143*, 4059.

(23) Cattarin, S.; Musiani, M. *Electrochem. Commun.* **2005**, *7*, 762.

(24) Higashi, G. S.; Becker, R. S.; Chabal, Y. J.; Becker, A. J. *Appl. Phys. Lett.* **1991**, *58*, 1656.

(25) Lewerenz, H. J.; Bitzer, T.; Gruyters, M.; Jacobi, K. *J. Electrochem. Soc.* **1993**, *140*, L44.

(26) Lewerenz, H. J.; Aggour, M.; Murrell, C.; Jakubowicz, J.; Kanis, M.; Campbell, S. A.; Cox, P. A.; Hoffmann, P.; Jungblut, H.; Schmeisser, D. *J. Electroanal. Chem.* **2003**, *540*, 3.

(27) Hassan, H. H.; Chazalviel, J.-N.; Neumann-Spallart, M.; Ozanam, F.; Etman, M. *J. Electroanal. Chem.* **1995**, *381*, 211.

(28) Hassan, H. H.; Fotouhi, B.; Sculfort, J.-L.; Abdel-Rehiem, S. S.; Etman, M.; Ozanam, F.; Chazalviel, J.-N. *J. Electroanal. Chem.* **1996**, *407*, 105.

(29) Searson, P. C.; Zhang, X. G. *Electrochim. Acta* **1991**, *36*, 499.

(30) Vanmaekelbergh, D.; Searson, P. C. *J. Electrochem. Soc.* **1994**, *141*, 697.

(31) Keddam, M.; Lizee, J.-F.; Pallotta, C.; Takenouti, H. *J. Electrochem. Soc.* **1984**, *131*, 2016.

(32) Ozanam, F.; Chazalviel, J.-N. *J. Electron Spectrosc. Relat. Phenom.* **1993**, *64/65*, 395.

(33) Iler, R. K. In *The Chemistry of Silica*; Wiley-Interscience: New York, 1979; Chapter 1.

(34) Bates, R. G. In *Determination of pH. Theory and Practice*; Wiley-Interscience: New York, 1973; Chapters 7−8.

(35) Bates, R. G.; Bennetto, H. P.; Sankar, M. *Anal. Chem.* **1980**, *52*, 1598.

(36) Eddowes, M. J. *J. Electroanal. Chem.* **1990**, *280*, 297.

(37) Da Fonseca, C.; Ozanam, F.; Chazalviel, J.-N. *Surf. Sci.* **1996**, *365*, 1.